Available online at www.sciencedirect.com
ScienceDirect
Proceedings of the Combustion Institute 32 (2009) 327–334
Proceedings of the Combustion Institute
www.elsevier.com/locate/proci

Formation and destruction of nitric oxide in methane flames doped with NO at atmospheric pressure

D.A. Knyazkov [a,*], A.G. Shmakov [a], I.V. Dyakov [b], O.P. Korobeinichev [a,c], J. De Ruyck [b], A.A. Konnov [b,d]

[a] Institute of Chemical Kinetics and Combustion, Novosibirsk, Russia
[b] Department of Mechanical Engineering, Vrije Universiteit Brussel, Brussels, Belgium
[c] Novosibirsk State University, Novosibirsk, Russia
[d] Department of Mechanical Engineering, Technische Universiteit Eindhoven, Eindhoven, The Netherlands

Abstract

A study of formation and destruction of NO in adiabatic laminar premixed flames of $CH_4 + O_2$ mixtures diluted with N_2 or Ar (with various dilution ratios) in a range of equivalence ratios at atmospheric pressure is presented. Nitric oxide was seeded into the flames using mixtures of diluent gas + 100 ppm of NO. The heat flux method was employed to measure adiabatic burning velocities of these flames. Nitric oxide concentrations in the post-flame zone at 10, 15 and 20 mm above the burner surface were measured using probe sampling. Burning velocities and NO concentrations simulated using a previously developed chemical kinetic mechanism were compared with the experimental results. The conversion ratio of NO seeded into the flames was determined. The kinetic mechanism accurately predicts burning velocities over the range of equivalence ratios and NO conversion in the rich flames. Significant discrepancies between measured and calculated NO conversion in the lean and near-stoichiometric flames were observed and discussed.

Keywords: Burning velocity; Nitric oxide; Laminar flame; NO conversion

1. Introduction

Exhaust Gas Recirculation (EGR) is considered as the basic method to control Homogeneous Charge Compression Ignition (HCCI) combustion [1]. The application of EGR in HCCI engines has a number of effects on the combustion process and emissions:

- preheating effect: the inlet charge temperature increases due to hot EGR gases;
- dilution effect: the introduction of the EGR gases leads to a reduction of the oxygen concentration;
- heat capacity effect: the total heat capacity of the mixture of the EGR gases, air, and fuel will be higher owing to the higher heat capacity of carbon dioxide and water vapor;
- chemical effect: unburned hydrocarbons, CO, CO_2, NO, H_2O, etc. in the EGR gases are chemically active and could moderately affect reaction rates.

* Corresponding author. Fax: +7 383 3307350.
E-mail address: knyazkov@kinetics.nsc.ru (D.A. Knyazkov).

1540-7489/$ - see front matter © 2009 The Combustion Institute. Published by Elsevier Inc. All rights reserved.
doi:10.1016/j.proci.2008.06.037

To address these effects and also NO reburning processes in flames, a number of studies have been performed in methane flames with admixture of NO at sub-atmospheric pressures [2–16] as well as at atmospheric and higher pressures [17–22].

A summary of experimental results obtained in premixed $CH_4 + O_2 + N_2 + NO$ flames at various conditions is given in Fig. 1, where conversion ratio of NO versus initial concentration of NO in the flames is plotted. Here, conversion ratio was determined as the ratio of destroyed [NO] to [NO] added initially to the fresh mixture. One can see that all experimental data were obtained in the flames with initial [NO] additive higher than 1000 ppm. Lean ($\phi = 0.86$) premixed $CH_4/O_2/N_2$ and $H_2/O_2/N_2$ flames stabilized on a McKenna burner at atmospheric pressure with addition of 0.11–0.33% of NH_3, NO and N_2O were studied by Martin and Brown [21]. Using microprobe gas sampling, relationships between NO and N_2O formation in the post-flame zone and addition of NH_3, NO and N_2O to combustion mixture were determined. The relative error of the measurements of NO concentration in the post-flame zone was about ±10–50%. The effect of addition of 1000 ppm of NO on the structure of premixed CH_4/air flames in a range of equivalence ratios 0.8–1.7 was studied by Jansohn et al. [18]. A nozzle burner was used for flame stabilization and concentrations of stable species were determined. A comparison of the measurements and modeling using the mechanism of Miller and Bowman [24] in the rich ($\phi = 1.25$) undoped flame showed an under-prediction of NO concentration in the post-flame zone by a factor of 2. On the other hand, in the flame seeded with 1000 ppm of NO the modeling over-predicted the NO concentration by a factor of 1.2 at the same experimental conditions. Feng et al. [22] studied the structure of burner-stabilized $CH_4/O_2/Ar$ flames doped with NO (960–1070 ppm) using a quartz microprobe sampling and subsequent chemiluminescence analysis. They found that the modeling using the mechanism of Lindstedt et al. [25] under-predicts NO concentrations in the post-flame zone at rich conditions ($\phi = 1.3$–1.4) by a factor of 1.5–2. In very rich flames ($\phi = 1.4$–1.7) and in lean ones ($\phi = 0.8$–1.0) the modeling however satisfactory predicts NO concentration.

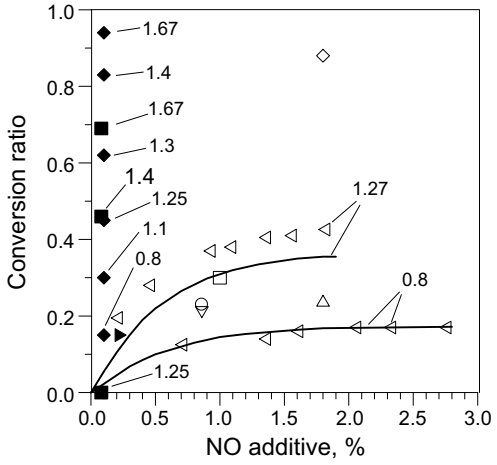

Fig. 1. Conversion ratio of nitric oxide in a number of $CH_4 + O_2 + N_2 + NO$ flames at various conditions derived from measurements obtained by different research groups. Filled squares: [18], equivalence ratios $\phi = 0.8$–1.66 (specified on the plot), pressure $p = 1$ atm; filled right triangle: [21], $\phi = 0.85$, $p = 1$ atm; filled diamonds: [22], $\phi = 0.8$–1.66 (specified on the plot), $p = 1$ atm; open diamond: [2], $\phi = 1$, $p = 10$ torr; open circle: [3], $\phi = 1$, $p = 10$ torr; open up triangle: [4], $\phi = 1$, $p = 10$ torr; open down triangle: [5], $\phi = 1$, $p = 10$ torr; open square: [6], $\phi = 1$, $p = 10$ torr; open left triangle: [23] (lines indicate modeling results obtained in this work), $\phi = 0.8$ and 1.27, $p = 25$–30 torr.

Measurements of NO conversion in the flames doped with lower concentration of nitric oxide were not reported. Numerical simulations, e.g. [7,17,19,23,26] based on the GRI-Mech. 2.11 [27], 3.0 [28], and Miller–Bowman kinetic mechanism [24] showed that in the lean flames doped with low concentration of NO (on the average less than ~600 ppm) its consumption does not exceed 10%. This fact was used for calibration of NO fluorescence signals in flames at atmospheric and higher [17,19], as well as at sub-atmospheric pressures [7,23,26]. Thomsen et al. [19] calibrated NO fluorescence signal in premixed lean ($\phi = 0.6$) $CH_4/O_2/N_2$ flames stabilized on a McKenna burner at pressures 1–14 atm with addition of 157 ppm of NO. They assumed that no NO is destroyed in the flame front of these flames, and validated their assumption by computer modeling, which predicted less than 5% NO destruction. Bessler et al. [17] performed their calibration using a lean premixed flame ($\phi = 0.95$) stabilized on a McKenna burner doped with NO (300–600 ppm). It was concluded that in this flame decomposition of NO additive was less than 10%.

Thus, the literature showed that the degree of NO reburning in flames depends on the stoichiometry and on initial concentration of NO seeded into fresh mixture. Although there was no direct experimental proof, it was generally accepted that small amounts of NO seeded into lean flames are not consumed (within ±10 %) and can be used for, e.g., LIF signal calibration.

The original goal of the present work was therefore to investigate NO reburning mostly in rich premixed methane flames at atmospheric pressure for validation of the Konnov detailed kinetic mechanism [29]. The heat flux method was used for flame stabilization. This method allows accurate measurements of the laminar burning velocities and facilitates comparison of

the measured concentrations of stable products with the modeling. During this study it was noticed that small amounts of NO seeded into $CH_4 + O_2 + N_2$ mixtures are consumed not only in rich, but also in lean flames. This unexpected finding motivated experiments in $CH_4 + O_2 + Ar$ flames to avoid interference of the NO natively formed from molecular nitrogen. In the following, these experimental results are presented and compared with the modeling; performance and deficiencies of the modeling are finally discussed.

2. Experimental details

Adiabatic flames were stabilized using the heat flux method [30] on a perforated plate burner of improved design [31], which has been a part of the experimental setup described elsewhere [32,33]. The temperature of the fresh gas mixture was controlled by a water cooling system in the burner's plenum chamber, and during the experiments it was maintained at 298 K.

In the present work, the flames of the mixtures of $CH_4 + O_2 + N_2$ seeded with NO and without additive, as well as of $CH_4 + O_2 + Ar + NO$ mixtures in a range of equivalence ratios were studied. The mixtures doped with NO were prepared using the mixture of N_2 or Ar with 100 ± 3 ppm addition of NO. All gases, including $N_2 + NO$ and $Ar + NO$ mixtures, were supplied by *Air Liquide*. The stated purity of methane, oxygen, nitrogen and argon were 99.995% or better. Two nitrogen diluted flames with the dilution factor $D = O_2/(O_2 + N_2)$ equal to 0.209 and 0.18 as well as argon diluted flame with $O_2/(O_2 + Ar)$ ratio of 0.17 were studied.

The methodology of the measurements of burning velocity was described in details earlier [30,32]. The experimental uncertainties in burning velocity measurements are mostly the results of the small random errors in gas velocities and the determination of the conditions of the zero net heat flux from the thermocouples measurement of temperature distribution on burner surface. A detailed analysis and quantification of burning velocity errors was reported earlier [32], and the overall accuracy of the burning velocity measurements was estimated to be better than ± 0.8 cm/s (double standard deviation with 95% confidence level). Concentration measurements were carried out using non-cooled quartz probe with inlet diameter of 0.9 mm, 6 mm external diameter and wall thickness of 1 mm. The sampled gas was ducted to the gas analyzers through a conditioning unit, a membrane pump and a filter. Water (dew point 5 °C) was removed from the gas sample in the conditioning unit by rapid chilling without dissolution of gas components in the liquid phase. As a consequence, the measured concentrations were compared to the modeling results recalculated to a dry basis. The probe used introduces gas-dynamic and thermal perturbations into the flame that may affect measured species concentrations. A detailed analysis of the errors associated with the probe influence on the measurements results (due to flame perturbation by the probe, conversion of the sampled gas in the probe, etc.), as well as sampling methodology were reported earlier [33]. To eliminate the probe effects in concentration measurements, we did not attempt to resolve spatial concentration profiles and performed sampling in the post-flame zone only. To measure nitric oxide concentration, the Fisher Rosemount Model 951A NO/NO_2 chemiluminescence analyzer was used. Before each set of measurements the sampling and analyzing system was calibrated with a mixture of 100 ppm of NO in nitrogen (or argon). Instrumental errors of the analyzer, and calibration procedure were discussed earlier [33]. In the present work, the measurements of NO or NO_x (the sum of NO and NO_2) were indistinguishable within the experimental accuracy. The flame modeling described below confirms that in the post-flame zone of interest the concentration of NO_2 was always below 0.5% of that of NO. However, a possible NO_2 formation from NO in the probe was not neglected. In the present work, the total concentration of NO_x was measured and attributed to the NO concentration in the post-flame zone. Taking into account all error sources, the uncertainty in the measurement of NO concentration was evaluated [33] to be always better than 10%. Sampling was performed at heights of 10, 15 and 20 mm above the burner surface. Simultaneously with [NO] measurements, the measurements of the concentrations of CO, CO_2 and O_2 were also carried out. Comparing them with the simulated [CO], [CO_2] and [O_2], the range of equivalence ratio, where the flame is less affected by the ambient air entrainment, was established according to the procedure used before [31,33,34]. The measurements of [NO] within this range only are presented below.

3. Modeling

A detailed C/H/N/O reaction mechanism for the combustion of small hydrocarbons was used for the modeling [29]. The current version of the mechanism consists of 1207 reactions among 127 species. This mechanism has been validated with experimental data available for oxidation, ignition, and flame structure of hydrogen, carbon monoxide, formaldehyde, methanol, methane, ethane, propane, and some of their mixtures [29,32,33]. The CHEMKIN II collection of codes [35,36], including transport properties [37] from Sandia National Laboratories, were used. Multicomponent diffusion and thermal diffusion

options were taken into account. Adaptive mesh parameters were GRAD = 0.1 and CURV = 0.5. Modeling of a flame structure was carried out taking into account downstream heat losses. For this purpose, the structure of the adiabatic flame was first modeled. Then, the calculated adiabatic temperature profile was modified downstream from the flame front assuming a constant temperature gradient of 100 K/cm as: $T_{x<0} = T_{ad}$, $T_{x>0} = T_{ad} - 100x$, where x is the axial distance from the flame front in cm. The temperature decrease due to the heat losses to the environment with the gradient as large as 100 K/cm was observed experimentally by van Maaren et al. [38,39]. These measurements were directly taken into account in approximation of the temperature profiles used in our calculations. Finally, the flame structure was simulated with the corrected temperature profile using the "burner-stabilized flame" option in the PREMIX code.

To analyze the reaction pathways of nitric oxide transformation in the flames, an investigation of N-element fluxes from species to species was performed using the KINALC code [40], a post-processor of the output files of the PREMIX code. Since the element flux analysis should be carried out with a reaction mechanism containing irreversible reactions only, the original mechanism [29] was first converted into the irreversible form by the MECHMOD code [41]. The Flux Viewer code [42] was used to visualize N-fluxes.

4. Results and discussion

Figure 2 shows adiabatic burning velocities measured at atmospheric pressure in the flames of $CH_4 + O_2$ mixtures diluted with both N_2 and Ar seeded with NO and without additive (for N_2 diluted flames). Simulated burning velocities in these flames are also presented. Modeling shows that the chemical kinetic mechanism accurately reproduces burning velocities of these flames in the whole range of equivalence ratios. One can see that NO additive does not result in appreciable change of the flame burning velocity within the experimental uncertainties. The modeling results also showed that within typical resolution of numerical calculations (±0.2 cm/s) addition of NO does not influence the flame burning velocity.

Figures 3 and 4 represent measured and calculated concentrations of NO (dry basis) as functions of equivalence ratio at 10, 15 and 20 mm above the burner surface in $CH_4/O_2/N_2$ flames ($D = 0.209$ and 0.18, respectively) without NO additive and doped with NO. A good qualitative agreement between experimental and numerical results is observed over the range of equivalence ratios for both doped and undoped flames. However, some quantitative discrepancies between the simulated and experimental data are evident. The model satisfactory reproduces the experimental data in both undoped flames over the range of equivalence ratios. In the flames doped with NO, the model overestimates NO concentrations in the lean mixtures.

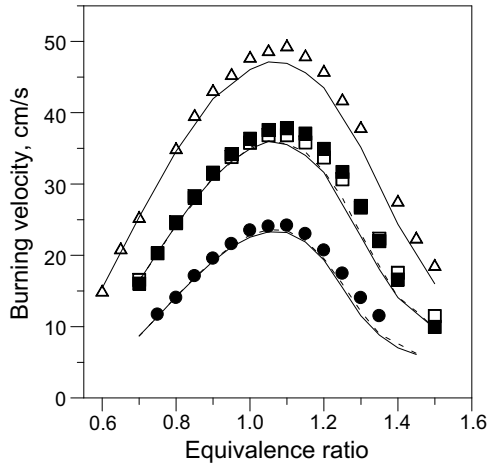

Fig. 2. Adiabatic burning velocities at atmospheric pressure and initial gas temperature of 298 K. Open symbols: measurements in NO-doped flames, solid symbols: measurements in undoped flames. Circles and squares: $CH_4 + O_2 + N_2$ flames with dilution factor $D = 0.18$ and 0.209, respectively; triangles: $CH_4 + O_2 +$ (Ar + NO) flames with $D = 0.17$. Lines: modeling, solid lines: NO-doped flames, dashed lines: undoped flames.

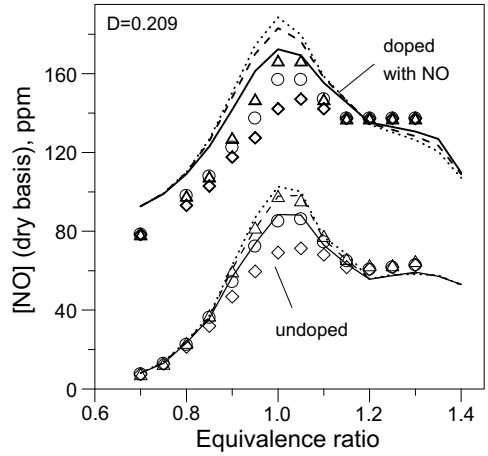

Fig. 3. Concentration of NO at different distances from the burner in post-flame zone of the flames of $CH_4 + O_2 + N_2$ mixtures ($D = 0.209$) doped with NO and undoped. Lines: modeling; symbols: experiment. Solid lines and diamonds: [NO] at 10 mm from the burner surface; dashed lines and circles: [NO] at 15 mm; fine dashed lines and triangles: [NO] at 20 mm.

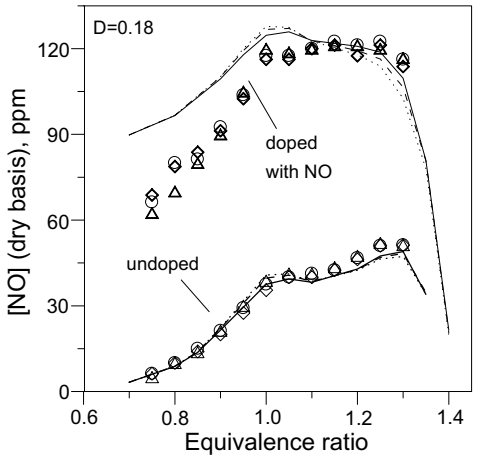

Fig. 4. Concentration of NO at different distances from the burner in post-flame zone of the flames of $CH_4 + O_2 + N_2$ mixtures ($D = 0.18$) doped with NO and undoped. Lines: modeling; symbols: experiment. Solid lines and diamonds: [NO] at 10 mm from the burner surface; dashed lines and circles: [NO] at 15 mm; fine dashed lines and triangles: [NO] at 20 mm.

Measured and calculated NO concentrations in the post-flame zone of $CH_4/O_2/(Ar + NO)$ flame ($D = 0.17$) are shown in Fig. 5. Calculated [NO] are in quite good agreement with the measured values in stoichiometric and rich flames regardless of a slight overestimation (by ~3 ppm). In the lean flames, serious discrepancy between simulated and measured [NO] is observed. Calculated [NO] are almost independent of equivalence ratio, whereas experimental values rapidly decrease with decreasing ϕ. Maximum difference (~23 ppm) between calculated and measured [NO] is at $\phi \approx 0.75$. One can see that the discrepancies between the measured and calculated [NO] are in excess of the measurement uncertainties discussed above as well as earlier [33]. Taking into account all error sources, the uncertainty in the measurement of NO concentration was evaluated [33] to be always better than 10%. Repetition of the experiments in methane + air flames [33] 6 years later on a perforated plate burner of improved design with new probes, gases and calibrating mixtures [31] revealed small differences in the measurements of [NO] not exceeding 3–5 ppm. In the present work, the comparison of the [NO] in flames without additive and doped with NO is much more straightforward, being performed at the same conditions within a few consecutive days. Therefore, the measurements of NO in the mixtures doped with NO are likely correct and the kinetic model appears to be responsible for these discrepancies.

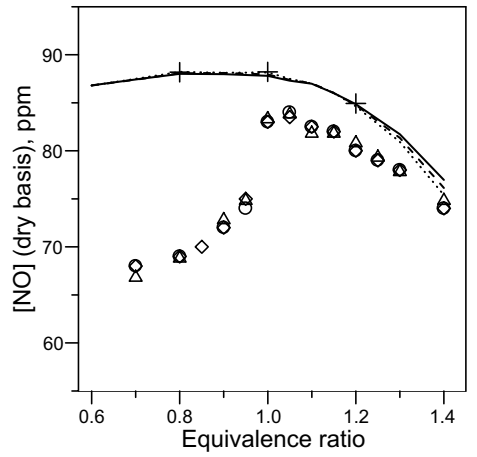

Fig. 5. Concentration of NO at different distances from the burner in post-flame zone of the flames of $CH_4 + O_2 + (Ar + NO)$ mixtures ($D = 0.17$). Lines: modeling; symbols: experiment. Solid lines and diamonds: [NO] at 10 mm from the burner surface; dashed lines and circles: [NO] at 15 mm; fine dashed lines and triangles: [NO] at 20 mm. Crosses are modeling with GRI 3.0 chemical kinetic mechanism.

The [NO] measurements given above can be represented in terms of NO conversion ratio, which is usually defined as Conv. ratio $= 1 - ([NO]_{dop} - [NO]_{undop})/[NO]_{add}$, where $[NO]_{dop}$ and $[NO]_{undop}$ are the NO concentrations in doped with NO and undoped flames, respectively, $[NO]_{add}$ is the NO concentration in initial combustion mixture. Though this definition in $CH_4/O_2/N_2$ flames assumes subtraction of the two values of the same order of magnitude thus increasing relative uncertainty, it addresses, on the other hand, concerns on the possible modification of the sample composition in the probe. At each equivalence ratio the composition of the gases in the non-cooled probe was the same with exception of the nitric oxide itself. Any systematic error caused by, e.g., surface reactions, would then be largely compensated. Figures 6–8 show the NO conversion ratio derived from the experimental and modeling results at different heights above the burner. The absolute error in determining the values of conversion ratio derived from the experiments is about ±0.06. Simulation results show that in near-stoichiometric and lean flames the nitric oxide originally present in the fresh mixture is consumed only slightly (NO conversion is close to zero), whereas in rich flames notable destruction of NO is observed. The model satisfactory reproduces the conversion ratio of NO in rich flames. However, contrary to the modeling results, experimental data show a considerable consumption of NO in near-stoichiometric and lean flames. In these flames, measured NO conversion ratio is about 0.2.

The occurrence of NO conversion in the rich flames is due to NO reburning processes, which were quite well studied earlier, e.g. [22,23]. An

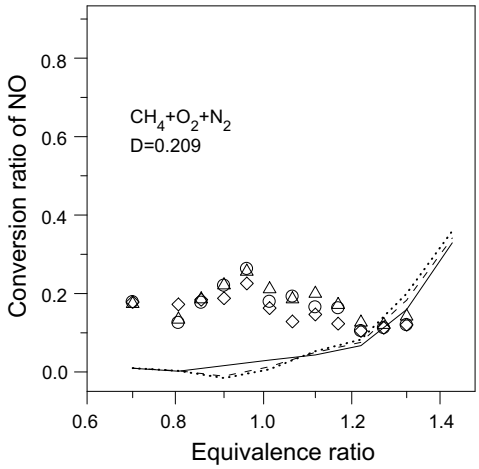

Fig. 6. Conversion ratio of NO in $CH_4 + O_2 + N_2$ flames doped with NO. Lines: modeling; symbols: measurements. Solid line and diamonds: at 10 mm above the burner; dashed lines and circles: at 15 mm; fine dashed lines and triangles: at 20 mm.

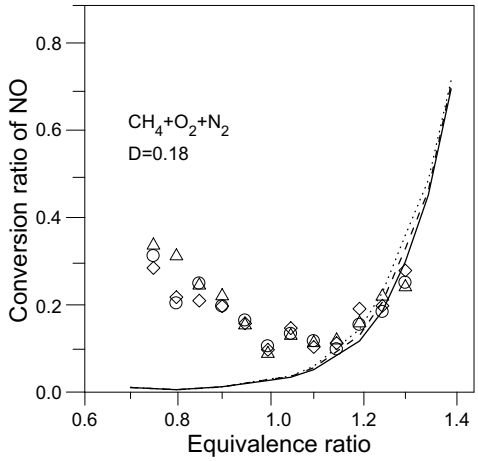

Fig. 7. Conversion ratio of NO in $CH_4 + O_2 + N_2$ flames doped with NO. Lines: modeling; symbols: measurements. Solid line and diamonds: at 10 mm above the burner; dashed lines and circles: at 15 mm; fine dashed lines and triangles: at 20 mm.

attention should be given to the fact that NO consumption in lean and near-stoichiometric flames is not predicted by the present, nor by other models [24,25,27,28], while it is observed experimentally. As evidence, in Figs. 5 and 8 we provide some values of NO concentration (at 15 mm above the burner surface) and conversion ratio calculated using GRI 3.0 mechanism [27] for $CH_4/O_2/(Ar + NO)$ flame. As can be seen, GRI-Mech. 3.0 is similar to the Konnov mechanism [29] in predicting concentration of NO in post-flame zone and NO conversion ratio. The results

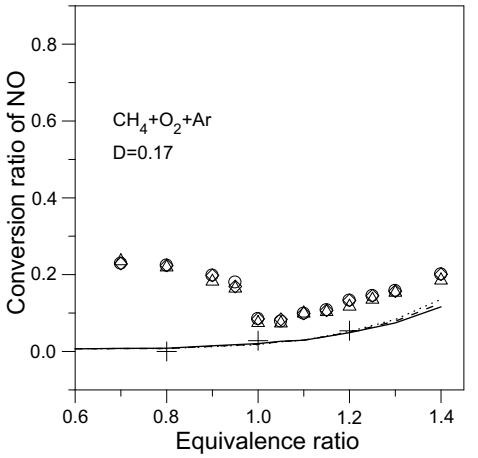

Fig. 8. Conversion ratio of NO in $CH_4 + O_2 + Ar$ flames doped with NO. Lines: modeling; symbols: measurements. Solid line and diamonds: at 10 mm above the burner; dashed lines and circles: at 15 mm; fine dashed lines and triangles: at 20 mm. Crosses are modeling with GRI 3.0 chemical kinetic mechanism.

obtained in the present work qualitatively agree with the experimental data available in the literature (see Fig. 1). The NO conversion ratio was found to depend strongly on both composition of initial gas mixture and concentration of NO additive (Fig. 1). For example, increasing the concentration of NO additive from 0.6% up to 3% gives the rise of conversion ratio in lean ($\phi = 0.8$) $CH_4/N_2/O_2$ flame from 12% up to 17% [23]. Modeling performed in that work also predicts approximately the same values of NO conversion ratio. However, it should be emphasized that in all studies mentioned in the introduction the concentration of NO additive were higher than about 1000 ppm.

One can conclude that the conversion of nitric oxide revealed experimentally in the present work in lean and near-stoichiometric flames doped with small amount of NO indicates drawbacks of the used kinetic model and other models, which demonstrate a near-zero NO conversion in the lean flames. To understand this discrepancy, the most important reaction pathways responsible for formation and destruction of NO in different combustion zones in lean and rich flames were analyzed. Figure 9 shows simulated spatial concentrations of NO as well as temperature profiles in lean ($\phi = 0.8$) and rich ($\phi = 1.3$) Ar-diluted flames seeded with NO. Modeling shows that NO additive has no effect on the temperature of the flames. Only the most relevant fragments of the NO profiles in flames are shown in Fig. 9. From the [NO] profiles one can distinguish several zones of consumption as well as production of NO in the flames. A specific feature of [NO] variation in both (lean and rich) flames is a fast NO

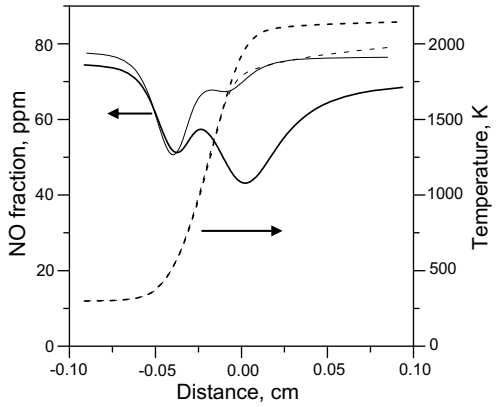

Fig. 9. Simulated spatial variation of NO concentration as well as temperature profiles in lean ($\phi = 0.8$, thin lines), and rich ($\phi = 1.3$, thick lines) Ar-diluted flames seeded with NO.

consumption in the preheat zone. In agreement with earlier observations [6,18], NO removal in this zone is the result of reactions $HO_2 + NO \leftrightarrow NO_2 + OH$ (1), $NO + OH(+M) \leftrightarrow HONO(+M)$ (2), $CH_3O + NO \leftrightarrow CH_2O + HNO$ (3) producing NO_2, HONO and HNO. Moving downstream, the concentration of nitric oxide drops to its first minimum and then begins to rise again in both flames. Although the removing of NO in this zone via reactions (1), (2) and (3) is reinforced by the termolecular reaction $CH_3 + NO(+M) \leftrightarrow CH_3NO(+M)$ (6), formation of NO dominates here because of reactions of accumulated NO_2 with H and CH_3 radicals ($NO_2 + H \leftrightarrow NO + OH$ (4) and $CH_3 + NO_2 \leftrightarrow CH_3O + NO$ (5)). Further downstream decrease of [NO], which is considerably more significant in the rich flame, is due to consumption of NO because of reactions with HCCO, CH_2 and CH_3 radicals yielding HCNO and HCN: $SCH_2 + NO \leftrightarrow HCN + OH$ (7), $HCCO + NO \leftrightarrow HCN + CO_2$ (8), $HCCO + NO \leftrightarrow HCNO + CO$ (9), $CH_3 + NO \leftrightarrow HCN + H_2O$ (10), $CH_2 + NO \leftrightarrow HCNO + H$ (11). NO is formed here primarily from NO_2, HONO, HNO and NH by the reactions (4), (5), (−2) and $HNO + H \leftrightarrow NO + H_2$ (12). In the post-flame zones of both lean and rich flames, NO formation is controlled by the reactions of HNO, NH, N with H, O and OH radicals.

This analysis shows that the key reactions responsible for production and destruction of nitric oxide at fuel-lean and rich conditions are mainly the same. To increase the predicted conversion ratio of NO in lean flames while keeping close performance of the mechanism in rich flames, the pre-exponential factors of rate constants of the key reactions discussed above were varied within tolerable limits. These tolerable limits comprise uncertainty of the pre-exponential factors themselves and of the activation energies. This did not bring significant improvement in the model behavior. One can also assume that some missing reactions between NO and radical species could be included into the mechanism in such a way that they are more operational in lean than in rich flames. Analyzing calculated concentration profiles of all species, it was found that the maximum difference in the peak concentrations of radicals in lean and in rich flames shown in Fig. 9 does not exceed a factor of 2. This difference is clearly insufficient to compensate significant discrepancy observed in, e.g., $CH_4/O_2/(Ar + NO)$ flames (Fig. 5), where over-prediction in lean flames (23 ppm) is almost an order of magnitude larger than in rich flames (3 ppm).

5. Conclusions

Burning velocity and probe sampling measurements of the concentrations of NO in the post-flame zone of laminar, premixed, non-stretched flames of $CH_4 + O_2$ mixtures diluted with N_2 or Ar doped with NO (100 ppm in diluent gas) and without additive were presented. The experimental data were compared with simulation results obtained using the Konnov detailed chemical kinetic mechanism. The model accurately reproduces laminar burning velocities in all flames. Using measured and predicted NO concentrations, the conversion ratio of NO was determined. Simulation results showed that in near-stoichiometric and lean flames the nitric oxide originally present in the fresh mixture is consumed only slightly, whereas in rich flames notable destruction of NO was observed. The model reproduces the conversion ratio of NO in rich flames. However, contrary to the calculation results, considerable consumption of NO (conversion ratio ~0.2) was observed experimentally in lean and near-stoichiometric flames. To understand a possible mechanism of NO consumption in the fuel-lean conditions, the most important reactions responsible for NO transformation in different combustion zones in lean and reach flames were analyzed. These reactions were found to be mostly the same in lean and rich conditions.

Acknowledgments

The Russian Foundation of Basic Research and Ministry of Flanders are acknowledged for the support of this work by the Grant No. 05-03-34815-MF-a and within the project BIL05/RU/76, respectively. The NATO and The Russian Science Support Foundation are acknowledged for the financial support of this work through the grants to I.V. Dyakov and to A.G. Shmakov, respectively.

References

[1] X.-C. Lu, W. Chen, Z. Huang, *Fuel* 84 (2005) 1084–1092.
[2] W. Juchmann, H. Latzel, D.I. Shin, et al., *Proc. Combust. Inst.* 27 (1998) 469–476.
[3] B.A. Williams, J.W. Fleming, *Combust. Flame* 98 (1994) 93–106.
[4] T. Etzkorn, S. Muris, J. Wolfrum, et al., *Proc. Combust. Inst.* 24 (1992) 925–932.
[5] B.A. Williams, J.W. Fleming, *Combust. Flame* 110 (1997) 1–13.
[6] B.A. Williams, L. Pasternack, *Combust. Flame* 111 (1997) 87–110.
[7] L. Gasnot, P. Desgroux, J.F. Pauwels, L.R. Sochet, *Combust. Flame* 117 (1999) 291–306.
[8] J. Luque, J.B. Jeffries, G.P. Smith, D.R. Crosley, J.J. Scherer, *Combust. Flame* 126 (2001) 1725–1735.
[9] X. Mercier, L. Pillier, A. Bakali, M. Carlier, J.-F. Pauwels, P. Desgroux, *Faraday Discuss.* 119 (2001) 305–319.
[10] I. Rahinov, N. Ditzian, V.A. Lozovsky, S. Cheskis, *Chem. Phys. Lett.* 352 (2002) 169–175.
[11] V.A. Lozovsky, I. Rahinov, N. Ditzian, S. Cheskis, *Faraday Discuss.* 119 (2001) 321–335.
[12] I. Rahinov, N. Ditzian, A. Goldman, S. Cheskis, *Proc. Combust. Inst.* 30 (2005) 1575–1582.
[13] S. Zabarnick, *Combust. Sci. Technol.* 83 (1–3) (1992) 115–134.
[14] J. Vandooren, J. Bian, P.J. Van Tiggelen, *Combust. Flame* 98 (4) (1994) 402–410.
[15] A. Garo, D. Puechberty, *Bull. Soc. Chim. Belg.* 99 (7) (1990) 473–481.
[16] A. Garo, C. Hilaire, D. Puechberty, *Combust. Sci. Technol.* 86 (1992) 87–103.
[17] W.G. Bessler, C. Schultz, T. Lee, et al., *Appl. Phys. B* 75 (2002) 97–102.
[18] P. Jansohn, J. Regnery, B. Lenze, *Gas Erdgas* 133 (8) (1992) 392–398.
[19] D.D. Thomsen, F.F. Kuligowski, N.M. Laurendeau, *Appl. Opt.* 36 (1997) 3244–3252.
[20] J.M. Goodings, G.B. De Brou, D.K. Bohme, *Can. J. Chem.* 59 (1981).
[21] R.J. Martin, N.J. Brown, *Combust. Flame* 80 (1990) 238–255.
[22] B. Feng, T. Ando, K. Okazaki, *JSME Int. J. B: Fluid Therm. Eng.* 41 (4) (1998) 959–965.
[23] P.A. Berg, G.P. Smith, J.B. Jeffries, D.R. Crosley, *Proc. Combust. Inst.* 27 (1998) 1377–1384.
[24] J.A. Miller, C.T. Bowman, *Prog. Energ. Combust. Sci.* 15 (4) (1989) 278–338.
[25] R.P. Lindstedt, F.C. Lockwood, M.A. Selim, *Combust. Sci. Technol.* 108 (4–6) (1995) 231–254.
[26] A.V. Mokhov, H.B. Levinsky, C.E. van der Meij, *Appl. Opt.* 36 (15) (1997) 3233–3243.
[27] C.T. Bowman, R.K Hanson, W.C. Gardiner, V. Lissianski, M. Frenklach, M. Goldenberg, G.P. Smith. Available from: <www.me.berkeley.edu/gri_mech/>.
[28] G.P. Smith, D.M. Golden, M. Frenklach, N.W. Moriarty, B. Eiteneer, M. Goldenberg, C.T. Bowman, R.K. Hanson, S. Song, C. William, J. Gardiner, V.V. Lissianski, Z. Qin. Available from: <http://www.me.berkeley.edu/gri_mech/>.
[29] A.A. Konnov, Detailed reaction mechanism for small hydrocarbons combustion. Release 0.5. Available from: <http://homepages.vub.ac.be/~akonnov/>.
[30] K.J. Bosschaart, L.P.H. de Goey, *Combust. Flame* 132 (2003) 170–180.
[31] F.H.V. Coppens, J. De Ruyck, A.A. Konnov, *Combust. Flame* 149 (2007) 409.
[32] I.V. Dyakov, A.A. Konnov, J. De Ruyck, K.J. Bosschaart, E.C.M. Brock, L.P.H. de Goey, *Combust. Sci. Technol.* 172 (2001) 81–96.
[33] A.A. Konnov, I.V. Dyakov, J. De Ruyck, *Combust. Sci. Technol.* 169 (2001) 127–153.
[34] I.V. Dyakov, J.D. Ruyck, A.A. Konnov, *Fuel* 86 (2007) 98–105.
[35] R.J. Kee, F.M. Rupley, J.A. Miller, Chemkin II: A Fortran Chemical Kinetics Package for the Analysis of Gas-Phase Chemical Kinetics, Report No. SAND89-8009, Sandia National Laboratories, 1989.
[36] R.J. Kee, J.F. Grcar, M.D. Smooke, J.A. Miller, A Program for Modeling Steady, Laminar, One-Dimensional Premixed Flames, Report No. SAND85-8240, Sandia National Laboratories, 1985.
[37] R.J. Kee, G. Dixon-Lewis, J. Warnatz, M.E. Coltrin, J.A. Miller, A Fortran Computer Code Package for the Evaluation of Gas-Phase Multicomponent Transport Properties, Report No. SAND86-8246, Sandia National Laboratories, 1986.
[38] A. van Maaren, L.P.H. de Goey, *Combust. Sci. Technol.* 99 (1994) 105–118.
[39] A. van Maaren, L.P.H. de Goey, R. van de Velde, in: K. Kuo (Ed.), *Non-Intrusive Combustion Diagnostics*, Begell House, New York, 1994, p. 544.
[40] T. Turanyi, I.G. Zsely, C. Frouzakis, KINALC: a CHEMKIN based program for kinetic analysis. Available from: <http://www.chem.leeds.ac.uk/Combustion/Combustion.html>.
[41] T. Turanyi, Mechmod v. 1.4: Program for the transformation of kinetic mechanisms. Available from: <http://www.chem.leeds.ac.uk/Combustion/Combustion.html>.
[42] I.G. Zsely, I. Virag, T. Turanyi, FluxViewer: visualisation tool for element fluxes. Available from: <http://garfield.chem.elte.hu/Combustion/fluxviewer.htm>.